



AN APPLICATION OF ARTIFICIAL NEURAL NETWORKS TO PISTON RING FRICTION LOSSES PREDICTION

Adolfo SENATORE¹, Sorin CIORTAN²

¹Department of Mechanical Engineering, University of Salerno, ITALY

²Department of Machine Design and Graphics,
“Dunarea de Jos” University of Galati, ROMANIA
sorin.ciortan@ugal.ro

ABSTRACT

A significant share of the total power loss in a modern automotive engine is due to the friction interaction between the piston ring pack and the cylinder wall. This paper presents the results of the simulations on the friction interaction top ring/cylinder wall in a SI engine taking into account the mixed lubrication (ML) regime and considering different engine operating conditions, lubricant viscosity, surface roughness. An Artificial Neural Network model and a procedure are presented in order to predict and optimise the friction losses. The ANN model allows for identifying the factors with the biggest influence on the friction loss evolution, while it can be used for finding the combinations of inputs factors leading to the lowest average friction coefficient value.

Keywords: piston ring, friction losses, artificial neural network

1. INTRODUCTION

The piston rings - cylinder wall interface is particularly critical as it has been estimated to account for 20% of the total engine mechanical loss (Figure 1) and it is extensively accepted that this kinematical pair provides substantial effects on wear, oil consumption and power loss in the internal combustion engine (ICE) [1-4]. The most common arrangement for a modern automotive internal combustion engine is a set of three rings (Figure 2).

Interesting applications of Neural Network based predictions have been applied in the tribology area in [5] for studying the behaviour of hydrodynamic thrust bearings with elastic bushing while, in another paper, the authors analyzed the motion characteristics of a rigid unbalanced rotor supported on elliptical bearings [6].

This paper introduces the results of simulations concerning the friction interaction top ring/cylinder wall of a SI engine taking into account a mixed lubrication (ML)

numerical model and an ANN algorithm in order to analyse the influence of factors, involved in piston rings - cylinder wall tribosystem functioning, on the friction losses evolution. The ANN models also allow for predicting the ring friction loss values.

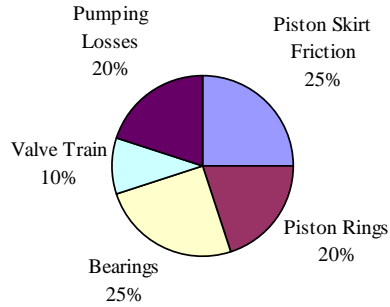


Fig. 1. Mechanical losses distribution in an ICE [1]

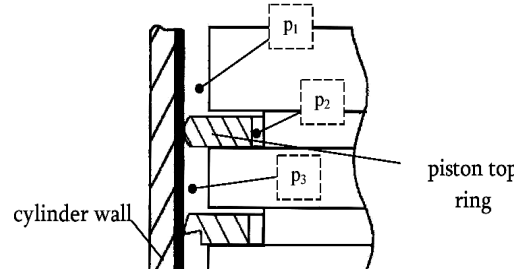


Fig. 2. Geometry of the tribosystem and gaps pressure

2. MODELING THE PISTON RING ML-REGIME

2.1. About Friction Characterizing a Mixt Regime

The implemented mathematical model is based on sharing the total load acting in the ring radial direction between the hydrodynamic lubrication (HDL) force and the solid-to-solid interactions along the asperities of the surfaces [7, 8, 9]:

$$F_R = F_C + F_H \quad (1)$$

with F_C the load carried by the interacting asperities and F_H the one carried by the hydrodynamic component. The total friction force, F_f , acting on the ring in tangential direction, is the sum of the friction force between the asperities and the shear force about the HDL regime:

$$F_f = \sum_{i=1}^{N_a} \iint_{A_{C_i}} \tau_{C_i} dA_{C_i} + \iint_{A_H} \tau_H dA_H \quad (2)$$

with N_a the number of asperities in contact, A_{C_i} the contact area of a single asperity i ; τ_{C_i} the shear stress at the asperity contact i ; A_H the contact area of the ring in HDL regime and τ_H the shear stress of this component.

The friction coefficient, f , can be calculated by the following equation:

$$f = \frac{F_f}{F_R} = \frac{F_{f,C} + F_{f,H}}{F_R} = \frac{\sum_{i=1}^{N_a} \iint_{A_{C_i}} \tau_{C_i} dA_{C_i} + \iint_{A_H} \tau_H dA_H}{F_R} \quad (3)$$

Both the components F_C and F_H show a strongly dependence on the height h_0 of the central point of the piston top ring (barrel shaped), i.e., the minimum nominal distance between the ring and the cylinder wall.

For the direct contact between the surfaces, the pressure generated by the deformation of the asperities is [8, 9]:

$$p_c(x) = \frac{2}{3} n \frac{1}{2} \frac{3}{2} \frac{1}{s} E' F_{3/2} \left(\frac{h(x)}{s} \right) \quad (4)$$

with $h(x)$ - the separation between the two surfaces, n - the density of the asperities on the area unit, β - the average radius of the asperities and σ_s - the standard deviation of the height distribution of the summits. The function $F_{3/2}$ is given by the following expression:

$$F_{3/2}(h) = \int_h^{\infty} (s-h)^{3/2} \phi(s) ds \quad (5)$$

where the ϕ function is the standardized height distribution of the summits, assumed given by the Gaussian distribution law (6); the relationship (7) allows for calculating the radial asperity force:

$$\phi(s) = \frac{1}{\sqrt{2\pi}} \text{Exp} \left(-\frac{1}{2} s^2 \right) \quad (6)$$

$$F_C = \int_0^B \int_0^L p_c(x) dx \quad (7)$$

The normal load due to the HDL regime and the shear stress due to the film lubricant have been calculated by integrating the Reynolds equation in the one-dimensional form, since the ring distance from the cylinder is evaluated with the axial-symmetry assumption.

$$\frac{\partial}{\partial x} \left(h^3 \frac{\partial p}{\partial x} \right) = 6\mu U \frac{\partial h}{\partial x} + 12\mu \frac{\partial h}{\partial t} \quad (8)$$

with the boundary conditions as in [10], with the data about the areas at p_1 , p_2 and p_3 (Fig. 2), from [11]. The viscous shear stresses are described by:

$$\tau_H(x) = -\mu \frac{U}{h(x)} + \frac{h(x)}{2} \frac{dp}{dx} \quad (9)$$

2.2. Numerical Algorithm

The data in Table 1 have been involved in all the simulations about the analysis of the friction behaviour of the considered piston ring. The algorithm has been implemented in MathematicaTM for calculating the function F_C versus h_0 with the chosen set of geometrical and material resistance data. Then, for the instantaneous values of the piston speed (U) and the pressure boundary conditions, the Reynolds equation is solved, in the unknown variable h_0 .

At each step of the numerical procedure, the crankshaft position θ is increased by a step ($5 \cdot 10^{-3}$ rad), the U value is updated as well as the pressure conditions from the indicated cycle; then, several iterations are performed on the HDL and asperities components for fulfilling the radial equilibrium condition with the algebraic constraint given by the total radial load F_R , i.e. the sum of the ring preload and the gas pressure on the ring back surface:

$$F_C(h_0) + F_H(h_0, U, p_1, p_3) - F_{R,t} - F_{R,g}(p_2) = 0 \quad (10)$$

The numerical simulations were carried out with the inter-ring gas pressures (see Figure 2) according to [11, 12] and the data in Table 1.

Once the previous equation has been solved and the minimum ring distance from the cylinder wall h_0 is known, the friction forces and the friction coefficient can be calculated using the above described relationships.

2.3. Simulations' data

Table 1. Parameters' matrix

Nr. crt.	Parameter	Symbol	Value	Unit
1.	Density of asperities	n	10^{11}	m^{-2}
2.	Average radius of asperities	β	10	μm
3.	Reduced modulus of elasticity	E'	231	GPa
4.	Standard deviation of the asperities	σ_s	0.10÷1.00	μm
5.	Length of the top ring	L_1	1.00÷2.00	mm
6.	Cylinder bore	B	60.0÷90.0	mm
7.	Ring slope	c	0.07÷0.12	-
8.	Ring radial preload	$F_{R,t}$	50÷150	N
9.	Oil viscosity	μ	5.0÷25.0	mPa s
10.	Maximum pressure of the indicated cycle	p_{max}	0÷50	bar
11.	Engine speed	N	1000÷5000	rpm
12.	Crank radius	R_C	33÷70	mm
13.	Characteristic ratio of the slider-crank mech.	L_{CR} / R_C	2.70÷3.60	-

2.4. Friction Mean Effective Pressure

The top ring friction work in a whole thermodynamic cycle (4π rad) is expressed by using the conventional friction mean effective pressure parameter (*f MEP*), i.e., the work divided by the displacement:

$$W_f = \int_{s=0}^{s=8R_C} F_f(s) ds = \int_0^{4\pi} F_f(\theta) \frac{U(\theta)}{\omega(\theta)} d\theta \quad (11)$$

$$f MEP = \frac{W_f}{V} = \frac{1}{\pi R^2 (2R_C)} \int_0^{4\pi} F_f(\theta) \frac{U(\theta)}{\omega(\theta)} d\theta \quad (12)$$

The values of *f MEP* in the following paper section are expressed in bar.

3. ARTIFICIAL NEURONAL NETWORK MODEL

In order to predict the friction coefficient values and to analyse the parameters influence on these values, an ANN model was developed. Because the functioning of ANN's is based on weights balance inside the neuron's network [13], different configurations of the model, obtained after different training cycles, can give different indications about the inputs influence on the output. On the other hand, multiples training cycles comparative studies on the same ANN model show that the differences occur only in values, the hierarchy being the same [14].

For the faults' elimination, the ANN model was developed using a genetic evolutionary algorithm provided by EasyNN software [15]. As input data, the parameters from Table 1 were used, leaving out the constant ones (lines 1, 2 and 3). As output data, the friction mean effective pressure values were considered. This way the model has ten inputs nodes and one output node.

The genetic evolutionary algorithm indicates that the best fitted architecture (presented in Figure 3) has twenty neurons organized in three layers, one hidden with nine neurons.

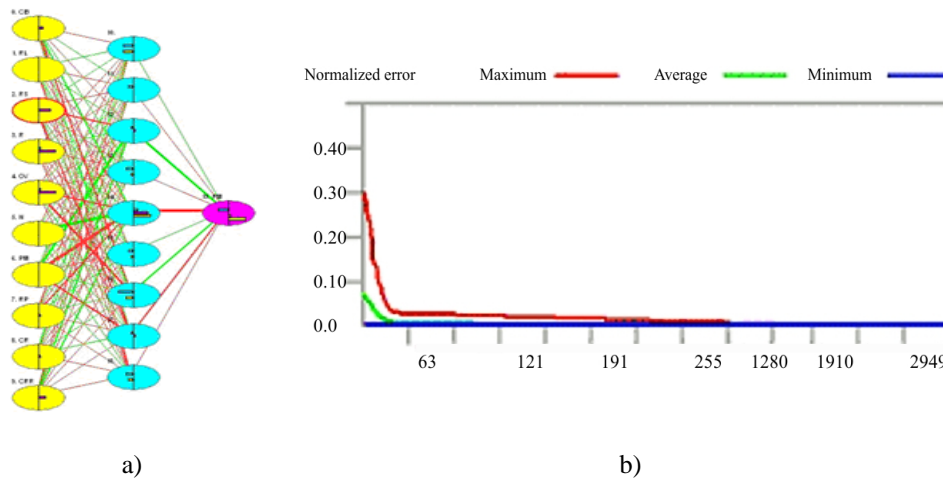


Fig. 3. The ANN model, a) the best fitted architecture, b) the learning graph

The targeted training error was 0.001 and the corresponding obtained validation scores were 100%.

As training data for the ANN model were used the results obtained by the mathematical model above described.

The trained model can be now used for predicting the friction coefficient values. The only condition is that the input values must remain in the corresponding ranges specified in Table 1.

Figure 4 presents a graphical comparison between the friction coefficient values predicted with the ANN model and the corresponding values calculated with the mathematical model.

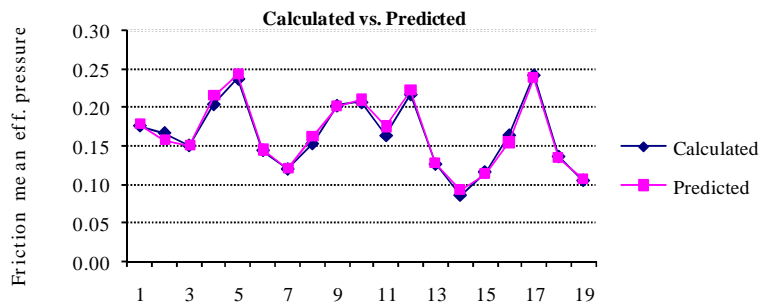


Fig. 4. The mathematical calculated friction mean effective pressure values versus the ANN predicted ones

The average correlation coefficient between the calculated values and the predicted ones of the friction coefficient is 0.9934, the predicted values being higher than

the calculated ones. In order to establish the influence hierarchy and the sensitivity of inputs parameters, several learning cycles were performed on the ANN model (the targeted learning error was 0.001 and the obtained validating scores were 100%).

Each learning cycle provides a graphical representation of inputs importance and sensitivity cycle (an examples is presented in figure 5). It can be observed that the hierarchy is the same for each learning cycle.

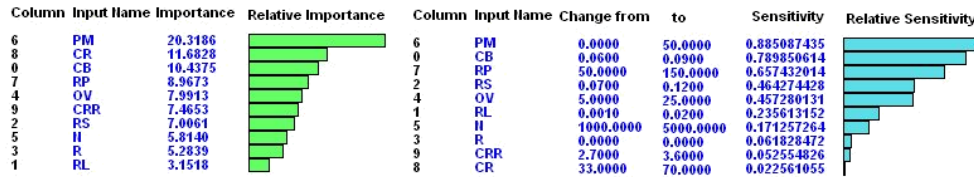


Fig. 5. The inputs importance and the sensitivity

Based on the obtained results an average numerical value for each input parameter was calculated, the results being presented in Table 2.

Table 2. The importance and the sensitivity of ANN inputs

Input name	Average importance values of ANN model [%]	Input name	Average sensitivity values of ANN model [%]
pmax	27	pmax	24
cylinder bore	15	cylinder bore	19
ring preload	13	ring preload	17
oil viscosity	11	oil viscosity	13
crank rod ratio	9	omega	10
ring slope	8	ring slope	9
omega	7	ring length	5
crank radius	6	roughness	3
roughness	5.5	crank rod ratio	2
ring length	5	crank radius	1

Based on the importance and the sensitivity analysis presented in Table 2, the most important parameters for the friction coefficient variation can be praised: *pmax*, *cylinder bore*, *ring preload* and *oil viscosity*. Varying the values of these ones, the lowest friction coefficient values can be predicted and obtained.

As a result, once the designers have defined the engine displacement and the overall geometry, the main influent factor is an operating condition, the pressure in the combustion chamber, i.e. the engine load, while the ring radial preload and slope are the specific ring design parameters on which more attention has to be devoted.

4. CONCLUSIONS

Based on the numerically obtained data, an ANN model for predicting and analysing the piston top ring friction losses was build.

The comparison between the ANN predicted values of the friction loss and the corresponding data obtained by the numerical algorithm shows a very good agreement with a correlation coefficient of 0.9934.

The ANN model allows also for identifying the factors with the biggest influence on friction loss evolution, while it can be used for finding the combinations of inputs factors leading to the lowest average friction coefficient value. The main advantage of using the ANN model is the possibility to predict the friction coefficient values for a given set of factors and to identify the way to minimize it.

Further applications will be studied in order to investigate more possibilities to reduce the friction losses in the top ring and other tribosystems in the internal combustion engines.

REFERENCES

- [1] **Taylor, C. M.**, 1998, Automobile engine Tribology - design considerations for efficiency and durability, *Wear*, 221, pp. 1-8.
- [2] **Dowson, D., Economou, P. N., Ruddy, B. L., Strachan, P. J. and Baker, A. J. S.**, 1979, Piston ring lubrication - Part II: theoretical analysis of a single ring and complete ring pack, *Proceedings of Energy Conservation through Fluid Film Lubrication Technology: Frontier in Research and Design*, ASME, New York, pp. 23-52.
- [3] **Taylor C. M.**, 1992, Fluid-Film Lubrication in the Internal Combustion Engines: an Invited Review, *J. Phys. D: Appl. Phys.* 25.
- [4] **Takiguchi, M., Machida, K., Furuhashi, S.**, 1988, Piston friction force of a small high speed gasoline engine, *J. of Tribology, ASME*, vol. 110(1), 112-8.
- [5] **Kurban, A.O., Yildirim S.**, 2003, Analysis of a hydrodynamic thrust bearing with elastic deformation using a recurrent neural network, *Tribology International*, 36, pp. 943-948.
- [6] **Qin P., Shen Y., Zhu J., Xu H.**, 2005, Dynamic analysis of hydrodynamic bearing-rotor system based on neural network, *International Journal of Engineering Science*, 43, pp. 520-531.
- [7] **Greenwood, J.A., Williamson, J.B.P.**, 1966, Contact of nominally flat surfaces, *Phil. Trans. R. Soc. London, Series A, Vol.19*, pp.295-300.
- [8] **Gelinck, E.R.M., Schipper, D.J.**, 2000, Calculation of Stribeck curves for line contacts, *Tribology International*, 33, pp. 175-181.
- [9] **Senatore, A., Ciortan, S.**, 2004, Oil ring friction loss simulation considering the mixed lubrication regime, *Proceedings of VAREHD 12, Int. Conf.*, October, Suceava (RO).
- [10] **D'Agostino, V., della Valle, S., Ruggiero, A., Senatore A.**, 2005, On the effective length of the top piston ring involved in hydrodynamic lubrication, *Lubrication Science*, Leaf Coppin – Vol. 17-3 (17) 309, pp. 309-318.
- [11] **Yun, J. E., Chung, Y., Chun, S. M., Lee, K. Y.**, 1995, An application of simplified average Reynolds equation for mixed lubrication analysis of piston ring assembly in an internal combustion engine, *SAE paper no. 952562*, SAE.
- [12] **D'Agostino, V., Senatore, A., Maresca, P.**, 2006, Theoretical analysis for friction losses minimization in piston rings, *Proc. of AITC 2006*, Parma (I), September 20-22.
- [13] **Haykin, S.**, 1994, Neural networks, a comprehensive foundation, Macmillan College Publishing Company, New York.
- [14] **Fujii, H., Mackay, D.J.C., Bhadeshia, H.K.D.H.**, 2004, Bayesian neural network analysis of fatigue crack growth rate in nichel base superalloys, *ISU International*, vol.3, no. 11, pp.1373-1382.
- [15] **EasyNN User Guide.**

Nomenclature

A_{Ci}	Area of a single asperity contact	p	Hydrodynamic pressure
A_H	Contact area of the hydrodynamic component	p_c	Asperities local contact pressure
B	Cylinder bore	p_{max}	Pressure peak of the indicated cycle
E'	Reduced modulus of elasticity	p_i	Pressure in the gaps (Fig. 2)
F_C	Normal load carried by the asperities	R	Piston radius
F_H	Normal load carried by the hydrodynamic component	R_C	Crankshaft radius
F_f	Ring friction force	U	Piston axial speed
F_R	Total normal load	V	Engine displacement per cylinder
$F_{R,t}$	Ring radial preload	x	Ring/Piston axial coordinate
$F_{R,g}$	Radial force due to the gas pressure p_2	β	Average asperities radius
$F_{3/2}$	Asperities height function	ϕ	Standardized height distribution
h	Oil film thickness	μ	Oil dynamic viscosity
h_0	Minimum ring distance from the cylinder wall	σ_s	Standard deviation of the asperities
L_{CR}	Connecting-rod length	τ_{ci}	Shear stress at the asperity contact
n	Density of asperities	τ_H	Shear stress of the hydrodynamic lubrication
N_a	Number of contacting asperities	ω, N	Engine speed (rad s^{-1} , rpm)